Geosci. Model Dev. Discuss., doi:10.5194/gmd-2016-188, 2016
Manuscript under review for journal Geosci. Model Dev.
Published: 31 August 2016

Geoscientific Model Development Discussions

Simulating climate warming scenarios with intentionally biased bootstrapping and its implications for precipitation

Taesam Lee

Dept. of Civil Engr., ERI, Gyeongsang National University,
501 Jinju-daero, Jinju, Gyeongnam, 660-701, South Korea

Corresponding Author: Taesam Lee, Ph.D.
Gyeongsang National University, Dept. of Civil Engineering
501 Jinju-daero, Jinju, Gyeongnam, 660-701, South Korea
Tel) +82-55-772-1797
Fax) + 82-55-772-1799
Email) tae3lee@gnu.ac.kr

Geosci. Model Dev. Discuss., doi:10.5194/gmd-2016-188, 2016
Manuscript under review for journal Geosci. Model Dev.
Published: 31 August 2016

Geoscientific Model Development Discussions

Abstract

The outputs from GCMs provide useful information about the rate and magnitude of future climate change. The temperature variable is the most reliable of the GCM outputs. However, hydrological variables (e.g., precipitation) from GCM outputs for future climate change possess an uncertainty that is too high for practical use. Therefore, a method, called intentionally biased bootstrapping (IBB), that simulates the increase of the temperature variable by a certain level as ascertained from observed global warming data is proposed. In addition, precipitation data was resampled by employing a block-wise sampling technique associated with the temperature simulation. In summary, a warming temperature scenario is simulated and the corresponding precipitation values whose time indices are the same as the one of the simulated warming temperature scenario. The proposed method was validated with annual precipitation data by truncating the recent years of the record. The proposed model was also employed to assess the future changes in seasonal precipitation in South Korea within a global warming scenario as well as in weekly time scale. The results illustrate that the proposed method is a good alternative for assessing the variation of hydrological variables such as precipitation under the warming condition.

Geosci. Model Dev. Discuss., doi:10.5194/gmd-2016-188, 2016
Manuscript under review for journal Geosci. Model Dev.
Published: 31 August 2016

1. Introduction

The complex influence of human actions on the climate system is well represented through global climate models (GCMs). A number of GCMs demonstrate variations in the large-scale atmospheric circulation and related changes in hydrometeorological variables (Allen and Ingram, 2002; Held and Soden, 2006; Lenderink and Van Meijgaard, 2008). It has been generally accepted that to quantify the range of possible changes in the hydrological cycle (such as precipitation and evaporation) is harder than in temperature (Allen and Ingram, 2002). Furthermore, hydrological variables vary much more in space and time than temperature and difficult to correctly simulate.

The relationship between temperature and precipitation has been studied in literature in order to predict the future variations of precipitation under the global warming condition. From the Clausius-Clapeyron (C-C) relation, saturation vapor pressure increases by 6-7% for each 1^{o}C increase in temperature and rainfall intensity should also increase at the same rate with warming (Trenberth and Shea, 2005). Lenderink and Van Meijgaard (2008) presented that 1hour intensity of precipitation exhibit a C-C relation for summer while showing super C-C scaling for winter.

These relations are only focused on very short time scale (not more than daily) or generally retrieved from GCM outputs. The behavior of mean precipitation over long-term period such as months and seasons is difficult to predict as temperature increases. It might be beneficial if one could derive the behavior of long-term mean precipitation under warming condition or the range of possible changes.

Therefore, a simple method that simulates temperature from observed data is proposed in the current study while increasing temperature up to a certain level as a warming scenario. In addition, precipitation is simulated by employing a block-wise resampling technique (Srinivas and

Geosci. Model Dev. Discuss., doi:10.5194/gmd-2016-188, 2016
Manuscript under review for journal Geosci. Model Dev.
Published: 31 August 2016

Srinivasan, 2000) associated with the temperature simulation. The resampled covariate, precipitation, forcing the warming condition in a certain level is obtained from the simulation. The proposed approach allows assessing the impact of precipitation as temperature increases with a current climate horizon.

The paper is organized as follows. In the next section, the fundamental mathematical background related to bias bootstrapping modeling is presented. The employed data and application methodology are described in section 3. The validation study of the proposed IBB approach is shown in section 4. The results assessing the long-term evolution of seasonal precipitation with simulating weekly temperature and precipitation data are illustrated in section 5. Finally, the summary and conclusions are presented in section 6.

2. Methodology

In order to simulate warming scenario, i.e. increasing mean temperature, up to a certain level, the observed data must be sampled with different combination. Intuitively, warmer temperature values are more likely to be resampled among the observations if the mean is increased. Therefore, the proposed method in the current study is to resample the observed data by fixing the mean temperature increment in the resampled dataset by weighting the probability of selection according to its magnitude (see Figure 1). In addition, the block bootstrapping with precipitation was employed to assess the changes in these variables as temperature increases.

2.1. Intentionally Biased Bootstrapping (IBB)

Bootstrapping (also known as resampling from observed data with replacement) is a statistical method for creating replica datasets from the original data to assess the variability of the quantities of interest without analytical calculation (Davison and Hinkley, 1997; Davison et al., 2003; Ouarda

Geosci. Model Dev. Discuss., doi:10.5194/gmd-2016-188, 2016
Manuscript under review for journal Geosci. Model Dev.
Published: 31 August 2016

and Ashkar, 1995). This bootstrapping technique has been extended to simulate time series of hydrometeorological variables (Beersma and Buishand, 2003; Lall et al., 1996; Lall and Sharma, 1996; Lee and Ouarda, 2011, 2010; Mehrotra and Sharma, 2005). In the current study, the intentionally bias bootstrapping (**IBB**) technique is employed so that the mean of the resampled datasets are varied as needed to simulate a global warming scenario.

IBB was proposed by Hall and Presnell (1999) as a class of weighted bootstrapping techniques in order to reduce bias or variance as well as to render some characteristic equal to a predetermined quantity. A good example of IBB is the adjustment of Nadaraya-Watson kernel estimators to make them competitive with local linear smoothing(Cai, 2001). In the current study, IBB was employed to simulate the temperature data from observation by bootstrapping under the constraint of increasing mean value, which indicates warming. The conceptual background of IBB has been employed to simulate future climates of weather analogs (Orlowsky et al., 2010; Orlowsky et al., 2008). In the current study, a IBB method with easy manipulation to simulate increased temperature data is proposed. The mathematical description of the proposed IBB method is the following.

Among an n number of observations x_i , where i=1,…,n, assume resampling the observations with replacement (i.e. bootstrapping) by increasing the mean of the simulated data by as much as Δ_μ; this implies that higher values have a higher probability of being resampled and lower values have lower selection probability. This IBB can be achieved by assigning different weights $S_{i,n}$ according to the magnitudes of the observations as

$$S_{i,n} = i / n \quad (1)$$

Geosci. Model Dev. Discuss., doi:10.5194/gmd-2016-188, 2016
Manuscript under review for journal Geosci. Model Dev.
Published: 31 August 2016

Geoscientific Model Development Discussions

Note that this assigned weight $S_{i,n}$ plays a role in the selection probability for the observed data in the IBB procedure after scaling and adjusting it.

The mean of the resampled data is

$$\tilde{\mu} = \frac{1}{\Psi}\sum_{i=1}^{n} S_{i,n} x_{(i)} \tag{2}$$

where $x_{(i)}$ represents the i^{th} increasing ordered value and $\Psi = \sum_{i=1}^{n} S_{i,n}$. The amount of the mean increase δ_{μ} is

$$\delta_{\mu} = \tilde{\mu} - \hat{\mu} = \frac{1}{\Psi}\sum_{i=1}^{n} S_{i,n} x_{(i)} - \frac{1}{n}\sum_{i=1}^{n} x_i \tag{3}$$

To obtain different values of δ_{μ},the weights can be generalized with the weight order (r) as

$$\tilde{\mu}(r) = \frac{1}{\Psi_r}\sum_{i=1}^{n} S_{i,n}^{r} x_{(i)} \tag{4}$$

where $\Psi_r = \sum_{i=1}^{n} S_{i,n}^{r}$. The difference is

$$\delta_{\mu}(r) = \tilde{\mu}(r) \quad \hat{\mu} = \frac{1}{\Psi_r}\sum_{j=1}^{n} S_{j,n}^{r} x_{(j)} - \frac{1}{n}\sum_{j=1}^{n} x_j \tag{5}$$

Once the magnitude of the mean increase is given (e.g., temperature increase) as Δ_{μ}, the weight order 'r' is estimated accordingly. For example, when the temperature change is obtained from the GCM outputs and this change is supposed to be propagated into a specific location and a finer

Geosci. Model Dev. Discuss., doi:10.5194/gmd-2016-188, 2016
Manuscript under review for journal Geosci. Model Dev.
Published: 31 August 2016

time scale, the selection of the weight order can be performed using a meta-heuristic optimization technique with the objective function as

$$\text{Minimize } [\Delta_\mu - \delta_\mu(r)]^2 \tag{6}$$

In the current study, the harmony search (HS) was used for the meta-heuristic optimization. The performance of the HS in hydrological applications is well reviewed in the literature (Geem et al., 2001; Lee and Geem, 2005, 2004; Lee and Jeong, 2014a; Mahdavi et al., 2007; Yoon et al., 2013a). Note that if $r > 0$, then $\delta_\mu(r) > 0$, which implies a global warming scenario; if $r < 0$, then $\delta_\mu(r) < 0$, which implies a global cooling scenario. When $r < 0$, lower values are resampled more frequently than are higher values. causing the mean of the resampled data to decrease. Furthermore, if r goes to infinity then the maximum of the observations is always selected, and if r goes to negative infinity, only the minimum is chosen.

In the IBB procedure, the adjusted scaled weight $\eta_i = S_{i,n}^r / \Psi_r$ is the probability that each i^{th} data point is subject to be selected. In the case of n=30, the weights for i=1,…,n are shown in Figure 2 with the weight order of r=0.5. The figure presents that the probability of being selected (i.e., η_i) is between approximately 0.01 for the lowest values and 0.05 for the highest order values of approximately 0.05 to lead positive bias in the resampled data (e.g., 1.0℃ increase). For example, if the number of the simulation is 100 and η_i=0.05, then the data point will be selected 5 times. A different probability implies a different number of selection for each data point. Subsequently, a different number of selections may lead to variation changes, called variance reduction or inflation. This issue is dealt with in the following section.

Geosci. Model Dev. Discuss., doi:10.5194/gmd-2016-188, 2016
Manuscript under review for journal Geosci. Model Dev.
Published: 31 August 2016

Geoscientific Model Development Discussions

2.2. Variance reduction and inflation

Because of the biased selection of higher values, the variance of the resampled data results is reduced (Lee and Jeong, 2014a; Lee and Ouarda, 2010; Lee et al., 2010a; Salas and Lee, 2010; Sharif and Burn, 2006). The estimated variance of the simulated data with IBB is

$$\tilde{\sigma}^2(r) = \sum_{j=1}^{n} \frac{S_{j,n}^{r}}{\Psi_r} x_{(j)}^{\ 2} - \tilde{\mu}^2 \tag{7}$$

Note that the variance in Eq. (7) is based on $\sigma^2 = E(X^2) - (EX)^2$. The difference of the variance is

$$\delta_{\sigma^2}(r) = \hat{\sigma}^2 - \tilde{\sigma}^2(r) \tag{8}$$

where $\hat{\sigma}^2$ is the sample variance of the observed data. To overcome the reduction of the variance in IBB, a random perturbation can be applied to the resampled data X_R as

$$X_R{}^* = X_R + \sqrt{\delta_{\sigma^2}(r)}\varepsilon \tag{9}$$

where ε is a random variable with a normal distribution $N(0,1)$. Subsequently, the mean and variance of the perturbed data are

$$\hat{\mu}_{R^*} = \tilde{\mu} \tag{10}$$

$$\hat{\sigma}_{R^*}^2 = \tilde{\sigma}^2 + \delta_{\sigma^2}(r) = \tilde{\sigma}^2 + \hat{\sigma}^2 - \tilde{\sigma}^2(r) = \hat{\sigma}^2 \tag{11}$$

2.3. Block bootstrapping

When the temperature presumably increases by a certain degree, it is interesting to note how the other weather variables vary. For example, if the temperature is increased by 1°C, the greatest

Geosci. Model Dev. Discuss., doi:10.5194/gmd-2016-188, 2016
Manuscript under review for journal Geosci. Model Dev.
Published: 31 August 2016

concern in climate research will be how the precipitation will change. To address this question, the block bootstrapping technique for the precipitation variable is adapted (Carlstein et al., 1998; Lee et al., 2010b). Once the temperature is resampled from the observed data at certain times using IBB, the observed precipitation data from the same time are considered (see Figure 2). Unlike for the case of temperature, there is no variance reduction in the resampled precipitation data because the precipitation data are not conditionally resampled. This block bootstrapping technique is popularly employed in multivariate weather simulations (Lee and Jeong, 2014b; Lee et al., 2012)..

2.4. Overall Simulation Procedure

The overall simulation procedure of temperature and precipitation data is described in this section. Simple schematic presentation of the procedure is shown in Figure 1.

Let x_i, y_i (i=1,…,n) be the observed temperature and precipitation data, respectively. Suppose that the simulation length is the same as the record length (i.e. n) and100 series need to be simulated.

(a) Assume that the increased overall temperature mean is known as Δ_μ.

(b) Estimate the weight order (r) from meta-heuristic algorithm (here, Harmony Search) with the objective function of Eq.(6) from the observed temperature data.

(c) Resample the temperature data from the observations with the probability of $S_{i,n}^{r}$ for i^{th} largest data (i=1,…, n).

(d) Assume that k^{th} largest temperature data $x_{(k)}$ is resampled from step (3) and its corresponding time index of (k) is 'j'. Note that (k) indicates the k^{th} largest value and j

Geosci. Model Dev. Discuss., doi:10.5194/gmd-2016-188, 2016
Manuscript under review for journal Geosci. Model Dev.
Published: 31 August 2016

indicates the j^{th} time-index value. Then, j^{th} precipitation data, y_j, is resampled simultaneously.

(e) Apply Eq.(9) to the resampled temperature data from step(3) (say, $x_{(k)} + \sqrt{\delta_{\sigma^2}(r)}\varepsilon$), if the variance inflation is chosen.

Note that the current procedure is explained for the case of no seasonal variability due to simplicity. In other words, the explained procedure above must be applied at each week or each month for weekly or monthly data. The detailed description of the proposed method for the case of monthly precipitation data with the full record is provided in the supplementary material (Supplement A).

3. Data description and application methodology

In the current study, weather stations that record temperature and precipitation in South Korea (74 locations) and that are managed by the Korea Meteorological Administration (KMA) were employed. South Korea is located in Far East Asia and has a mean annual precipitation of 1283 mm. This country is climatologically influenced by the Siberian air mass during winter and the Maritime Pacific High during summer. Most of the annual precipitation in South Korea falls during the rainy season from June to September due to the occurrence of tropical cyclones, extratropical cyclones, fronts and other weather systems. Because the orographic area in South Korea is heterogeneous and large, the rainfall in South Korea has large spatial and temporal variability (Park et al., 2007; Yoon et al., 2013b). The water resource control system, including climate change, is an important aspect of this study due to the seasonal and spatial variability of rainfall in this country.

Geosci. Model Dev. Discuss., doi:10.5194/gmd-2016-188, 2016
Manuscript under review for journal Geosci. Model Dev.
Published: 31 August 2016

Datasets shorter than 30 years of data were excluded, after which a total of 54 datasets were employed. The data were extracted from the KMA website (http://www.kma.go.kr/). Most of the time spans are approximately 33 years, from 1976 to 2008.

The validation study was performed with annual dataset to present the performance of the proposed model with truncating recent years as 1994-2008. The truncated data was not used in simulation but employed in comparison. Also, a case study was applied with the weekly dataset of the 54 stations in South Korea. In the application study of the proposed IBB procedure in section 5, (1) 0.5°C and 1.0°C increases in the mean weekly temperature were assumed; (2) weekly temperature datasets were simulated using the assumed temperature increase; (3) weekly precipitation datasets were also simulated along with the weekly temperature dataset as a block. Note that the simulation does include not a gradual change, such as a trend, but the overall mean change. We simulated the weekly time scale so that the data spanned a long enough period to provide a summary of weather statistics and a short enough period to reflect the temporal variability. Furthermore, the observed weekly datasets of temperature and precipitation were aggregated into seasonal time scale data, and the aggregated seasonal data were used to present the seasonal variations in precipitation as temperature increases.

Note that although we simulated the temperature with a specific condition of increase (e.g. +0.5 °C or +1.0°C), no such restriction was placed on the precipitation, allowing one to determine whether there is any change in precipitation with the condition of increasing temperature. One hundred series were simulated with the same time span as the observations.

Geosci. Model Dev. Discuss., doi:10.5194/gmd-2016-188, 2016
Manuscript under review for journal Geosci. Model Dev.
Published: 31 August 2016

Geoscientific Model Development Discussions

4. Validating IBB model with annual data

To further obtain the credibility of the proposed IBB model, we validated the model with truncating the last 15 years (1994-2008) of the annual mean temperature and precipitation data over South Korea. The last truncated 15 years were set as the validation period while the rest of the preceding years as the test period. The dataset of the test period was employed in simulation while the dataset of the validation period is only used in comparison to check how much the proposed model performs. Among others, annual scale data is employed to easily illustrate the performance of the proposed IBB model. At first, some mathematical terms need to be defined to explain the validation procedure as follows.

$$D\mu_p^{obs} = \mu p_V - \mu p_T \tag{12}$$

$$D\mu_p^{IBB} = \mu p_{IBB} - \mu p_T \tag{13}$$

where μp_V and μp_T are the mean annual precipitation over the validation years and over the test period, respectively, while μp_{IBB} is the annual mean precipitation of the IBB simulated data with the record length of the validation years. The same denotation as the precipitation variable is taken for the temperature variable as μT_V, μT_T, μT_{IBB}, $D\mu_T^{obs}$, and $D\mu_T^{IBB}$.

The validation procedure is (1) to truncate the 15 years (1994-2008) of annual temperature and precipitation for each station; (2) to estimate the mean differences of the annual temperature and precipitation between the validation period (1994-2008) and the test period (1976-1993), $D\mu_T^{obs}$ and $D\mu_p^{obs}$, respectively; (3) to perform the IBB simulation with the annual precipitation and temperature of the test period conditioned on the estimated mean differences of the temperature

Geosci. Model Dev. Discuss., doi:10.5194/gmd-2016-188, 2016
Manuscript under review for journal Geosci. Model Dev.
Published: 31 August 2016

Geoscientific Model Development Discussions

between two periods (i.e. $D\mu_T^{obs}$) for each station; and (4) to compare the estimated mean differences of the observed precipitation (i.e. $D\mu_p^{obs}$) with the mean differences between the IBB simulated precipitation and the precipitation for the test period (i.e. $D\mu_p^{IBB}$).

The annual mean temperature differences between the validation period and the test period at each station is presented in Figure 3 for the IBB simulated data ($D\mu_T^{IBB}$, boxplot) and the observed data ($D\mu_T^{obs}$, circle). The figure indicates that the IBB model fairly well simulates the temperature data as much as it was intended, except few stations that shows high increase especially with more than one-degree increase (e.g. stations 6 and 7). Note that the employed test period is relatively short and not enough number of high values of annual temperature is included during the test period and this might result the underestimation of the intended temperature increase.

In Figure 4, the annual mean precipitation of the observation over the validation period (μp_V, filled blue circle) and the test period (μp_T, filled red triangle) as well as the IBB simulation (μp_{IBB}, boxplot) is illustrated. The result indicates that the observed mean precipitation over the validation period (μp_V) presents higher than the mean for the test period (μp_T) in most of the stations. The IBB simulated data reflects this tendency showing higher mean precipitation than the mean precipitation of the test period though its magnitude shows some difference.

The mean of the observed annual precipitation for the validation period at each station and the mean of one hundred IBB simulated data is presented in Figure 5. The top panel presents that the simulated data fairly well reproduce the observed mean of annual precipitation for the validation period (1994-2008). The observed mean difference ($D\mu_p^{obs}$) of the annual precipitation

Geosci. Model Dev. Discuss., doi:10.5194/gmd-2016-188, 2016
Manuscript under review for journal Geosci. Model Dev.
Published: 31 August 2016

between the test period (1976-1993) and the validation period shown at the bottom panel of Figure 5 fairly matches with the one of the IBB simulated data ($D\mu_p^{IBB}$). Rather high variability at the difference is inevitable due to relatively small record length for both the test period and the validation period. Overall, the validation study implicates that the proposed IBB approach can simulate the future evolution of annual precipitation over South Korea.

In Figure 6, the spatial distribution of the differences for the annual mean precipitation is presented with the observed data (i.e. $D\mu_p^{obs}$) and with the IBB simulated data ($D\mu_p^{IBB}$). High increase of annual mean precipitation in the north and south part of the country and small increase and slight decrease in the south part shown in the observed data (left panel) is well reflected in the IBB simulated data (right panel) except that the increase is shown from the IBB simulated data (right panel) in the left south part of the country is not shown in the observed data. Overall, the figure indicates that the spatial pattern of the annual mean precipitation difference from the observed data (see the left panel) is similar to the one from the IBB simulated data (see the right panel).

5. Precipitation changes according to assumed temperature increase

Figure 7 shows the results of the fitted IBB model for the Buan station, located at 35° 44' N and 126° 43' E. The top panel (Figure 7(a)) shows the estimated weight order of each week for the mean temperature data employing the HS meta-heuristic algorithm with the objective function of Eq. (6) while assuming a 0.5℃ increase. The estimated values range from 0.2 to 1.3. The mean and standard deviation of the observed and theoretical results (see Eqs. (2) and (7)) with a 0.5℃ mean increase are shown in Figure 7(b) and (c), respectively. The predominant annual cycle of the

Geosci. Model Dev. Discuss., doi:10.5194/gmd-2016-188, 2016
Manuscript under review for journal Geosci. Model Dev.
Published: 31 August 2016

mean weekly temperature is seen in the mean statistics, as shown in Figure 7(b), while the annual cycle of the standard deviation (equivalent to the square root of variance) is not as prominent as the annual cycle of the mean (see Figure 7(c)). Note that the weight order and the standard deviation (see Figure 7(a) and (c)) are highly negatively correlated. In other words, when the standard deviation is small (e.g., at approximately the 23rd week), the weight order is high and vice versa. This result is intuitive in that if the variance is great, the corresponding temperature values differ greatly from each other. Subsequently, the weights of the large values to be selected are not necessarily much different from the weights of the low values in such a case, which induces a low weight order. In Figure 7(c), the variance difference between the observed and theoretical data, as defined in Eq. (8), is shown with a dotted line. This variance difference is inflated to the resampled data, as in Eq. (9). This inflation procedure is optional in assessing the overall trend of annual mean precipitation data regarding climate warming scenarios. However, it might be helpful when the purpose of the study is to evaluate an overall variation of extreme precipitation statistics.

The statistics of the simulated data from IBB with the condition of a 0.5°C degree mean temperature increase are shown as a boxplot in Figure 8; the statistics of the observed data are shown in the same figure with dotted lines and cross marks. The mean increases by exactly 0.5°C, as intended, and the standard deviation (square root of variance) is well preserved through the variance inflation process (see Eq. (8)). The minima and maxima of the mean weekly temperatures are increased.

Shown in Figure 9(a) are the mean differences between the simulated and observed weekly precipitation with the conditions of 0.5°C and 1.0°C increases at the Buan station. The differences

Geosci. Model Dev. Discuss., doi:10.5194/gmd-2016-188, 2016
Manuscript under review for journal Geosci. Model Dev.
Published: 31 August 2016

306 are not significant at the 5% level. However, the mean differences are continuously positive from
307 the 30th to 40th week, which is during the summer season. This result indicates that a seasonal
308 effect on the precipitation change must exist. Therefore, we also extended our study to a seasonal
309 time scale. The mean precipitation differences of all 54 stations are shown for 0.5°C and 1.0°C
310 increases in Figure 9(b) and (c), respectively. Both plots show a decrease in autumn and increases
311 in the other seasons.

312 For a 1.0°C temperature increase, 61%, 24%, and 45% of the employed stations show a
313 significant increase in mean precipitation for the winter, spring, and summer seasons, respectively.
314 In contrast, the mean temperature decreases during the autumn season. Approximately 30% of the
315 stations experience a significant change in the mean precipitation at the 5% level given a 1.0°C
316 temperature increase. The detailed information is provided in Table 1.

317 The spatial distribution of seasonal mean precipitation differences is presented in Figure 10
318 given the condition of a 1°C temperature increase. An increasing pattern of precipitation during
319 winter (see Figure 10(a)) can be seen over the South Korea peninsula. Notably, the eastern and
320 southern coastal areas undergo a significant increase with a 95% confidence interval (±5.38). Note
321 that the significance interval at each station is different because the variances between stations are
322 different. The detailed significance interval for each station is provided in Table 2. During spring
323 (see Figure 10(b)), the northern part of the country shows an increasing pattern while the
324 southwestern and southeastern parts show decreasing patterns, but their magnitudes are not
325 significant (±15.04). The summer precipitation (see Figure 10(c)) undergoes a significant increase
326 in the southwest area of the country (±29.94). In contrast to the other seasons, a significant decrease

Geosci. Model Dev. Discuss., doi:10.5194/gmd-2016-188, 2016
Manuscript under review for journal Geosci. Model Dev.
Published: 31 August 2016

in mean precipitation occurs during autumn (see Figure 10(d)) throughout the country, especially over the eastern coastal area. The same spatial pattern of seasonal mean precipitation can be observed given the condition of a 0.5°C temperature increase, as in the case of a 1.0°C temperature increase, with little significant change (see Figure 11).

The spatial distributions of seasonal precipitation changes seem to be related to the flow direction of the seasonal air mass. In South Korea, winter is influenced primarily by the Siberian air mass with prevailing northwesterly winds, while summer is hot and humid with southeasterly winds.

6. Summary and Conclusions

A simple method is proposed (1) to simulate precipitation given the condition of a mean temperature increase derived from the observations and (2) to address the problem of how the precipitation vary while the temperature is increased through global warming. The results illustrated that a simple IBB technique for the temperature variable incorporating block sampling of precipitation can achieve this objective.

The presented technique is valuable because hydrometeorological variables such as precipitation and discharge are difficult to model with current GCMs, while the temperature prediction is relatively accurate. The proposed method can be extended to other hydrometeorological variables as well as other applications, including studies at the global scale. The limit of the proposed method is that the temperature increase is limited since employed data is observational. One possibility for allowing a greater temperature increase than that from the observations is to include neighboring, similar stations or seasons. The author believes that the

Geosci. Model Dev. Discuss., doi:10.5194/gmd-2016-188, 2016
Manuscript under review for journal Geosci. Model Dev.
Published: 31 August 2016

348 proposed model can be a good surrogate or competitor in GCM-based climate change impact
349 assessments of hydrometeorological variables.

350 7. Code and Data Availability

351 All the employed code can be provided upon the request to the author of the current study. The
352 employed precipitation and temperature data over South Korea can be downloaded from the KMA
353 website http://www.kma.go.kr/weather/climate/past_cal.jsp .

354 Acknowledgements

355 This work was supported by the National Research Foundation of Korea (NRF) grant funded by
356 the Korean government (MEST) (No. 2015R1A1A1A05001007). All the employed data can be
357 provided upon the request to the author of the current study.

358

359

Geosci. Model Dev. Discuss., doi:10.5194/gmd-2016-188, 2016
Manuscript under review for journal Geosci. Model Dev.
Published: 31 August 2016

References

Allen, M. R. and Ingram, W. J.: Constraints on future changes in climate and the hydrologic cycle, Nature, 419, 224-232, 2002.

Beersma, J. J. and Buishand, T. A.: Multi-site simulation of daily precipitation and temperature conditional on the atmospheric circulation, Climate Research, 25, 121-133, 2003.

Cai, Z.: Weighted Nadaraya-Watson regression estimation, Statistics and Probability Letters, 51, 307-318, 2001.

Carlstein, E., Do, K. A., Hall, P., Hesterberg, T., and Kunsch, H. R.: Matched-block bootstrap for dependent data, Bernoulli, 4, 305-328, 1998.

Davison, A. C. and Hinkley, D. V.: Bootstrap Methods and their Application, Cambridge University Press, Cambridge, 1997.

Davison, A. C., Hinkley, D. V., and Young, G. A.: Recent Developments in Bootstrap Methodology, Statistical Science, 18, 141-157, 2003.

Geem, Z. W., Kim, J. H., and Loganathan, G. V.: A new heuristic optimization algorithm: Harmony search, Simulation, 76, 60-68, 2001.

Hall, P. and Presnell, B.: Intentionally biased bootstrap methods, Journal of the Royal Statistical Society. Series B: Statistical Methodology, 61, 143-158, 1999.

Held, I. M. and Soden, B. J.: Robust responses of the hydrological cycle to global warming, Journal of Climate, 19, 5686-5699, 2006.

380 Lall, U., Rajagopalan, B., and Tarboton, D. G.: A nonparametric wet/dry spell model for
381 resampling daily precipitation, Water Resources Research, 32, 2803-2823, 1996.

382 Lall, U. and Sharma, A.: A nearest neighbor bootstrap for resampling hydrologic time series, Water
383 Resources Research, 32, 679-693, 1996.

384 Lee, K. S. and Geem, Z. W.: A new meta-heuristic algorithm for continuous engineering
385 optimization: Harmony search theory and practice, Computer Methods in Applied Mechanics and
386 Engineering, 194, 3902-3933, 2005.

387 Lee, K. S. and Geem, Z. W.: A new structural optimization method based on the harmony search
388 algorithm, Computers and Structures, 82, 781-798, 2004.

389 Lee, T. and Jeong, C.: Frequency analysis of nonidentically distributed hydrometeorological
390 extremes associated with large-scale climate variability applied to South Korea, Journal of Applied
391 Meteorology and Climatology, 53, 1193-1212, 2014a.

392 Lee, T. and Jeong, C.: Nonparametric statistical temporal downscaling of daily precipitation to
393 hourly precipitation and implications for climate change scenarios, Journal of Hydrology, 510,
394 182-196, 2014b.

395 Lee, T. and Ouarda, T. B. M. J.: Identification of model order and number of neighbors for k-
396 nearest neighbor resampling, Journal of Hydrology, 404, 136-145, 2011.

397 Lee, T. and Ouarda, T. B. M. J.: Long-term prediction of precipitation and hydrologic extremes
398 with nonstationary oscillation processes, Journal of Geophysical Research D: Atmospheres, 115,
399 2010.

400 Lee, T., Ouarda, T. B. M. J., and Jeong, C.: Nonparametric multivariate weather generator and an
401 extreme value theory for bandwidth selection, Journal of Hydrology, 452-453, 161-171, 2012.

402 Lee, T., Salas, J. D., and Prairie, J.: An enhanced nonparametric streamflow disaggregation model
403 with genetic algorithm, Water Resources Research, 46, 2010a.

404 Lee, T., Salas, J. D., and Prairie, J.: An Enhanced Nonparametric Streamflow Disaggregation
405 Model with Genetic Algorithm, Water Resources Research, 46, W08545, 2010b.

406 Lenderink, G. and Van Meijgaard, E.: Increase in hourly precipitation extremes beyond
407 expectations from temperature changes, Nature Geoscience, 1, 511-514, 2008.

408 Mahdavi, M., Fesanghary, M., and Damangir, E.: An improved harmony search algorithm for
409 solving optimization problems, Applied Mathematics and Computation, 188, 1567-1579, 2007.

410 Mehrotra, R. and Sharma, A.: A nonparametric nonhomogeneous hidden Markov model for
411 downscaling of multisite daily rainfall occurrences, Journal of Geophysical Research-
412 Atmospheres, 110, D16108, 2005.

413 Orlowsky, B., Bothe, O., Fraedrich, K., Gerstengarbe, F. W., and Zhu, X.: Future climates from
414 bias-bootstrapped weather analogs: An application to the Yangtze River basin, Journal of Climate,
415 23, 3509-3524, 2010.

416 Orlowsky, B., Gerstengarbe, F. W., and Werner, P. C.: A resampling scheme for regional climate
417 simulations and its performance compared to a dynamical RCM, Theor. Appl. Climatol., 92, 209-
418 223, 2008.

419 Ouarda, T. B. M. J. and Ashkar, F.: Bootstrap-based intercomparison of regional flood estimation
420 procedures, Waterpower '95 - Proceedings of the International Conference on Hydropower, Vols
421 1-3, 1995. 2466-2475, 1995.

422 Park, J. H., Kang, B. S., Lee, G. S., and Lee, E. R.: Flood Runoff Analysis using Radar Rainfall
423 and Vflo Model for Namgang Dam Watershed, Journal of the Korean Association of Geographic
424 Information Studies, 10, 13-21, 2007.

425 Salas, J. D. and Lee, T.: Nonparametric Simulation of Single-Site Seasonal Streamflows, Journal
426 of Hydrologic Engineering, 15, 284-296, 2010.

427 Sharif, M. and Burn, D. H.: Simulating climate change scenarios using an improved K-nearest
428 neighbor model, Journal of Hydrology, 325, 179-196, 2006.

429 Srinivas, V. V. and Srinivasan, K.: Post-blackening approach for modeling dependent annual
430 streamflows, Journal of Hydrology, 230, 86-126, 2000.

431 Trenberth, K. E. and Shea, D. J.: Relationships between precipitation and surface temperature,
432 Geophysical Research Letters, 32, 1-4, 2005.

433 Yoon, S., Jeong, C., and Lee, T.: Application of Harmony Search to Design Storm Estimation from
434 Probability Distribution Models, Journal of Applied Mathematics, 2013, 11, 2013a.

435 Yoon, S., Jeong, C., and Lee, T.: Flood flow simulation using CMAX radar rainfall estimates in
436 orographic basins, Meteorol. Appl., doi: 10.1002/met.1382, 2013b. 2013b.

437

438

Geosci. Model Dev. Discuss., doi:10.5194/gmd-2016-188, 2016
Manuscript under review for journal Geosci. Model Dev.
Published: 31 August 2016

Geoscientific Model Development Discussions

439 Table 1. Mean precipitation difference of the observed and simulated data for seasonal data over

440 all the employed stations in South Korea in case of +1.0 °C mean temperature increase.

	Mean Diff					Mean Diff			
Station	Winter	Spring	Summer	Autumn	Station	Winter	Spring	Summer	Autumn
1	**11.2**	**14.3**	20.2	-12.0	28	2.6	12.1	9.6	-4.1
2	3.2	**22.4**	4.5	0.0	29	**4.4**	**20.6**	**50.4**	-3.8
3	11.0	5.0	21.5	**-17.2**	30	**5.5**	11.7	30.0	-4.2
4	1.6	**15.7**	**38.1**	-2.3	31	**4.4**	**19.2**	15.8	-4.7
5	1.5	11.9	3.9	-6.2	32	4.2	**15.9**	18.0	-2.0
6	1.7	10.1	**28.5**	-2.0	33	**6.6**	**16.4**	**46.1**	-4.2
7	1.7	8.2	16.8	-2.3	34	**9.5**	9.5	**32.6**	**-7.1**
8	3.2	**22.3**	33.6	-3.1	35	**6.4**	1.7	**44.1**	-6.8
9	2.3	**19.1**	**15.0**	-4.9	36	5.1	-4.2	**52.1**	**-9.4**
10	**9.8**	6.7	21.4	**-16.3**	37	**5.6**	7.4	**39.9**	**-9.4**
11	2.8	**18.8**	**30.3**	-3.3	38	**9.2**	-4.3	**53.8**	-3.1
12	5.3	10.8	**32.9**	-7.2	39	**9.6**	-3.2	**65.0**	-5.6
13	**5.1**	3.5	21.5	**-9.3**	40	**11.5**	-9.9	**82.2**	-6.5
14	**9.8**	1.2	28.8	-4.5	41	**9.1**	4.2	**33.3**	**-7.4**
15	**6.6**	-0.9	11.5	**-5.1**	42	**9.6**	-11.5	**61.2**	**-8.1**
16	**5.9**	-1.0	**32.6**	**-7.5**	43	4.2	12.9	**42.7**	-3.0
17	**10.2**	-9.3	26.7	0.6	44	**6.3**	**20.2**	**33.8**	-2.6
18	**8.2**	-1.7	**50.2**	-4.5	45	**12.9**	8.8	10.5	**-7.9**
19	**13.2**	-2.7	23.4	0.8	46	**5.8**	**11.2**	19.4	-3.8
20	**9.8**	-4.3	33.1	-0.7	47	3.1	**14.3**	**56.3**	**-7.0**
21	**8.1**	-15.4	12.4	-4.5	48	**7.1**	-2.4	14.8	**-4.7**
22	**7.8**	-6.0	**52.3**	-2.3	49	**9.0**	3.4	**68.4**	**-5.9**
23	**11.4**	-17.5	19.7	**-12.6**	50	4.2	2.1	31.6	-2.3
24	1.9	11.2	21.1	0.1	51	**8.9**	5.5	**39.5**	-3.2
25	2.3	8.6	21.8	-2.4	52	**8.6**	8.0	**78.2**	-1.5
26	2.3	8.8	13.4	0.8	53	**16.4**	6.0	28.8	-4.1
27	2.5	9.3	26.0	-2.9	54	**10.5**	20.9	23.2	1.7
Mean confidence interval						±5.38	±15.04	±29.94	±7.01
# of Significant Stations						33	13	25	16
(percent)						(61%)	(24%)	(46%)	(30%)

441

442
443

444

Geosci. Model Dev. Discuss., doi:10.5194/gmd-2016-188, 2016
Manuscript under review for journal Geosci. Model Dev.
Published: 31 August 2016

Geoscientific Model Development Discussions

445 Table 2. Confidence interval for mean precipitation difference of the observed and simulated data
446 for seasonal data.

Station	Winter	Spring	Summer	Autumn	Station	Winter	Spring	Summer	Autumn
1	10.7	12.4	28.4	13.6	28	3.89	14.15	32.45	6.08
2	3.7	13.2	29.0	5.1	29	4.71	14.76	31.49	6.34
3	12.7	10.3	29.6	14.2	30	5.24	14.79	30.39	5.55
4	3.7	14.6	34.7	7.6	31	4.08	14.26	27.61	7.45
5	3.6	12.0	25.9	7.8	32	4.25	14.31	28.31	7.09
6	4.0	12.0	25.3	5.6	33	5.00	15.87	31.29	8.08
7	3.6	14.0	25.9	7.7	34	5.62	13.73	25.75	6.06
8	4.1	13.7	26.4	6.4	35	4.86	12.44	30.64	6.93
9	4.1	14.8	27.1	8.6	36	5.61	12.53	27.52	7.52
10	8.9	10.5	26.7	11.4	37	5.32	12.89	26.21	7.28
11	4.8	14.5	23.0	7.0	38	5.12	13.53	32.37	5.46
12	5.5	15.2	30.7	6.4	39	5.15	15.64	34.46	6.45
13	4.6	13.1	24.6	5.2	40	5.27	20.28	37.15	6.87
14	8.2	12.9	30.9	6.7	41	4.80	20.76	29.50	5.57
15	4.8	12.1	23.6	4.5	42	5.20	21.00	35.75	7.88
16	5.6	12.5	26.9	6.3	43	4.45	15.73	26.47	6.16
17	7.2	15.7	30.1	6.9	44	5.23	14.63	26.25	5.11
18	5.2	15.4	31.9	5.7	45	8.23	11.25	24.05	7.16
19	6.9	20.1	35.1	8.7	46	4.30	10.81	24.10	4.29
20	6.0	19.3	34.3	7.5	47	4.60	11.30	25.36	4.91
21	4.6	15.7	26.5	6.1	48	4.80	11.24	23.40	4.32
22	5.0	19.5	30.1	6.9	49	5.81	12.41	34.88	5.73
23	5.4	22.6	39.4	8.4	50	5.38	14.71	33.37	5.54
24	3.6	17.3	27.5	8.3	51	4.73	15.29	30.09	6.00
25	3.6	13.1	30.8	6.6	52	6.32	17.35	41.62	7.15
26	4.0	13.5	28.2	6.9	53	7.70	29.41	44.00	11.16
27	3.3	13.5	27.7	4.6	54	7.56	23.95	42.12	9.89

447

448

Geosci. Model Dev. Discuss., doi:10.5194/gmd-2016-188, 2016
Manuscript under review for journal Geosci. Model Dev.
Published: 31 August 2016

Geoscientific Model Development Discussions

449

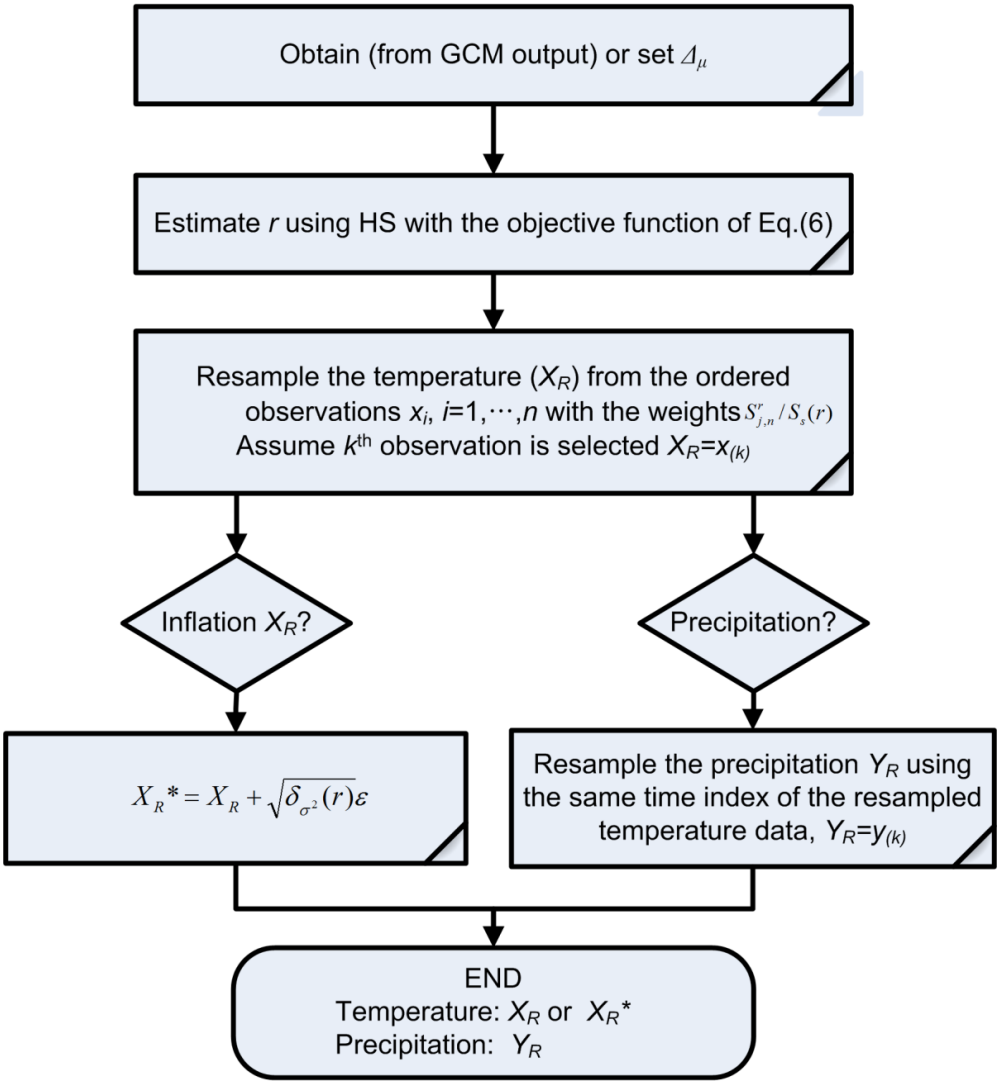

450

451 Figure 1. Procedure for the proposed simulation IBB method of temperature and precipitation data.

452

Geosci. Model Dev. Discuss., doi:10.5194/gmd-2016-188, 2016
Manuscript under review for journal Geosci. Model Dev.
Published: 31 August 2016

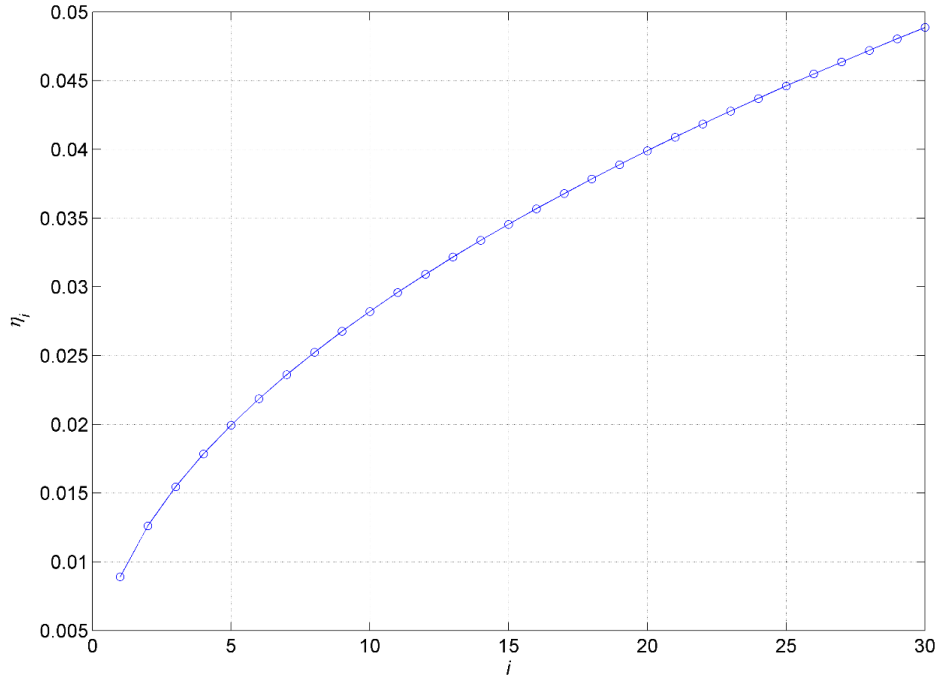

453

454 Figure 2. Example of the adjusted scaled weights (η_i) vs. order numbers in the case of n=30 and
455 order weight r=0.5. Note that η_i is the probability of being selected and increases as the order is
456 increased, so that higher values are subject to being selected more often than are lower values,
457 leading to a positive bias.

458

Geosci. Model Dev. Discuss., doi:10.5194/gmd-2016-188, 2016
Manuscript under review for journal Geosci. Model Dev.
Published: 31 August 2016

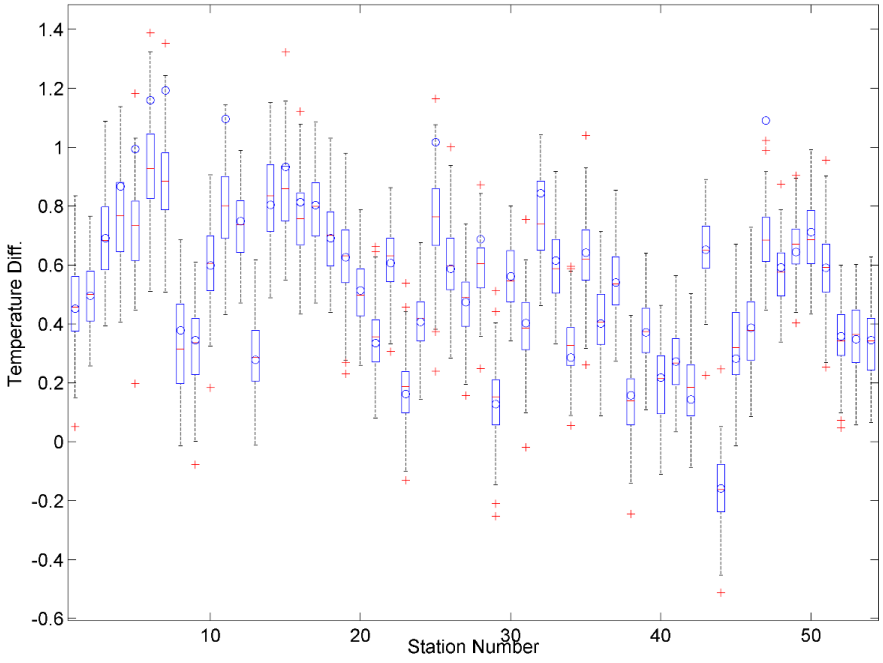

Figure 3. Annual mean temperature difference between the validation period (1994-2008) and the test period (1976-1993) for each station for the IBB simulated data (boxplot) and the observed data (circle). Boxes indicate the interquartile range (IQR), and whiskers extend to +/- 1.5IQR. The horizontal lines inside the boxes depict the median of the data. Data beyond the fences (+/-1.5IQR) are indicated by a plus symbol (+), which represent outliers.

Geosci. Model Dev. Discuss., doi:10.5194/gmd-2016-188, 2016
Manuscript under review for journal Geosci. Model Dev.
Published: 31 August 2016

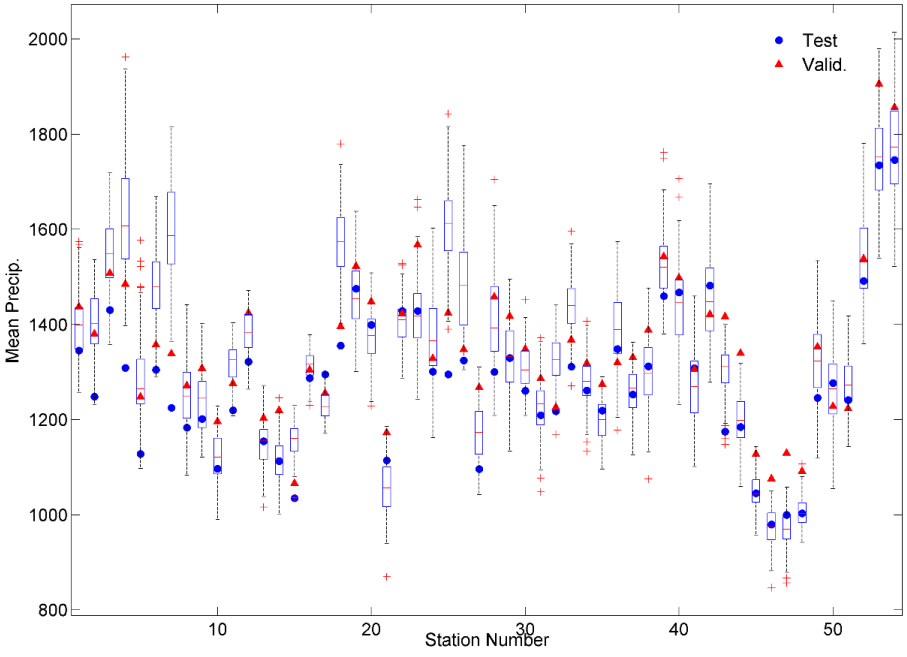

Figure 4. Annual mean precipitation of the IBB simulation (boxplot) and the observation over the validation period (filled blue circle) as well as the test period (filled red triangle) conditioned with the temperature change (see Figure 3). Note that the observed mean precipitation over the validation period (1994-2008) (see the red triangles) shows mostly higher than the mean over the test period (1976-1993) (see the blue circles). Also, the IBB simulated precipitation (boxplot) reflects this tendency showing higher than the mean precipitation of the test period (blue circles). Boxes indicate the interquartile range (IQR), and whiskers extend to +/-1.5IQR. The horizontal lines inside the boxes depict the median of the data. Data beyond the fences (+/-1.5IQR) are indicated by a plus symbol (+), which represent outliers.

Geosci. Model Dev. Discuss., doi:10.5194/gmd-2016-188, 2016
Manuscript under review for journal Geosci. Model Dev.
Published: 31 August 2016

Geoscientific Model Development Discussions
Open Access
EGU

476

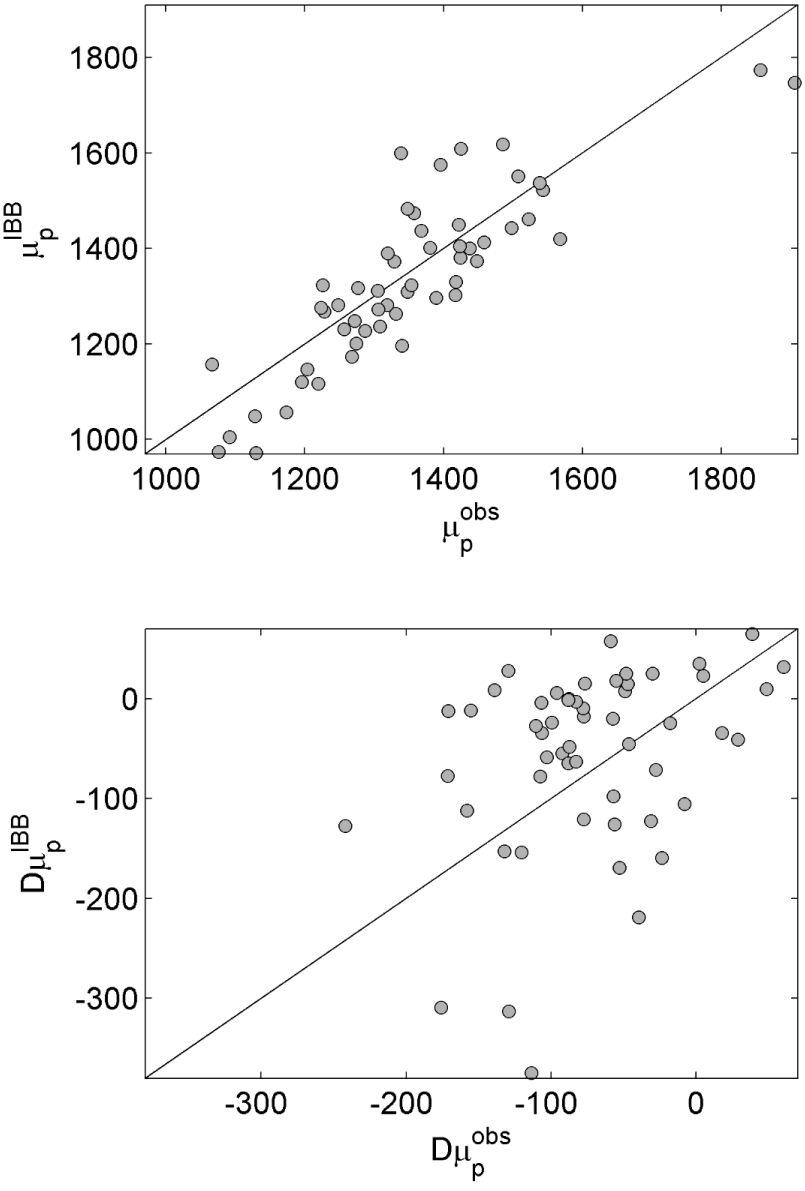

477
478 Figure 5. Annual mean precipitation (top panel) during the validation period (1994-2008) and its
479 difference (bottom panel) with the test period (1976-1993) for the observed data (abscissa) and
480 the IBB simulated data (ordinate) over all the employed stations in South Korea. For more details
481 about the difference at the bottom panel, see Eqs. (12) and (13).

Geosci. Model Dev. Discuss., doi:10.5194/gmd-2016-188, 2016
Manuscript under review for journal Geosci. Model Dev.
Published: 31 August 2016

Geoscientific Model Development Discussions
Open Access
EGU

482

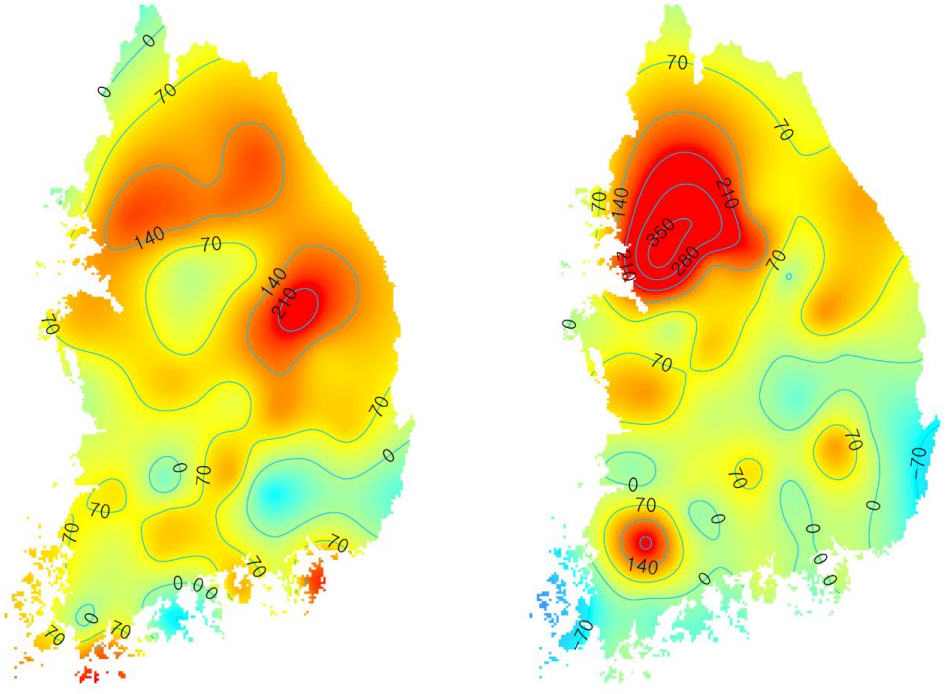

483

484 Figure 6. Spatial distributions of annual mean precipitation difference between the validation
485 period (1994-2008) and the test period (1976-1993) for the observed data (left panel) and the
486 IBB simulated data (right panel).

487

488

Geosci. Model Dev. Discuss., doi:10.5194/gmd-2016-188, 2016
Manuscript under review for journal Geosci. Model Dev.
Published: 31 August 2016

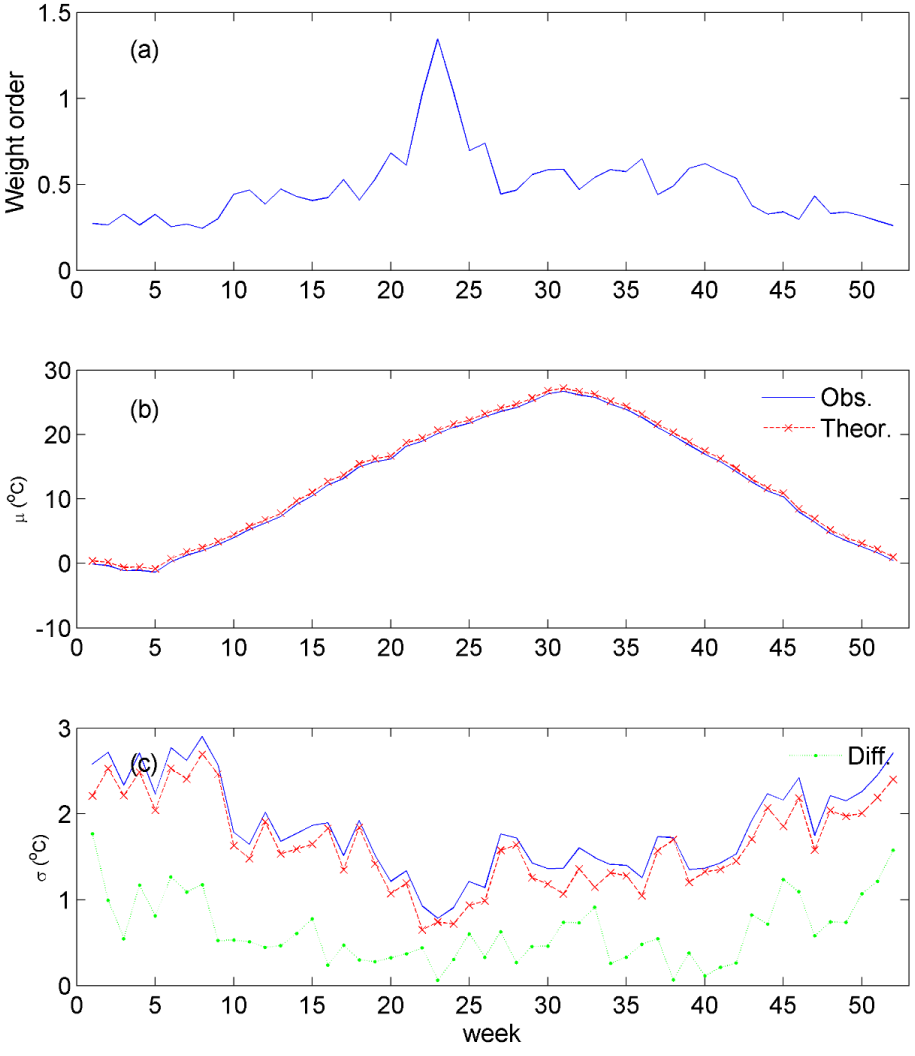

489

490 Figure 7. (a) Estimated weight order from HS and weekly statistics of (b) mean and (c) variance
491 for the observed temperature data (solid line) and the theoretical statistics (dashed line with cross)
492 using Eqs. (2) and (7) for Buan station. The weekly difference in variance between observation
493 and theoretical (see Eq. (8)) is shown in panel (c) by a dotted line.

494

Geosci. Model Dev. Discuss., doi:10.5194/gmd-2016-188, 2016
Manuscript under review for journal Geosci. Model Dev.
Published: 31 August 2016

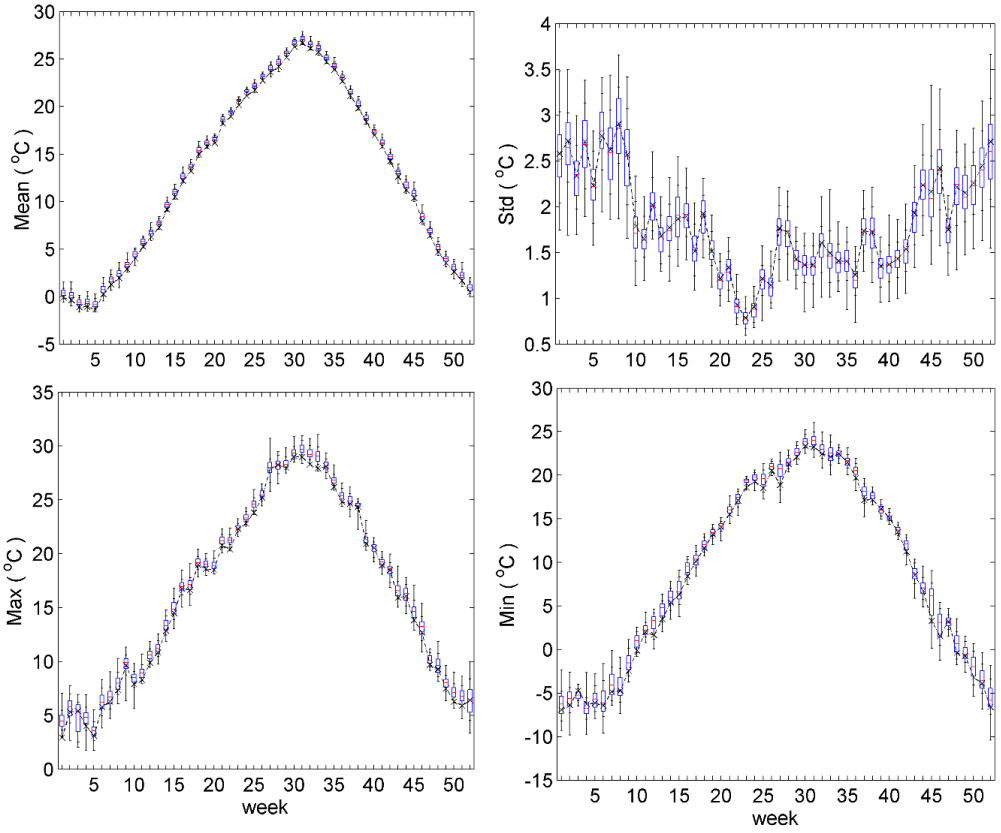

Figure 8. The statistics of the observed (dotted line with cross) and generated (boxplot) data for the weekly mean temperature using IBB with a 0.5°C temperature increase in Buan, South Korea. Boxes display the interquartile range (IQR), and whiskers extend to the extrema (i.e., maximum and minimum). The horizontal lines inside the boxes depict the median of the data. Note that the mean and maximum of the simulated data are increased significantly compared with the corresponding observed data, while the minimum of the simulated data is slightly increased and the standard deviation of the simulated data agrees with that of the observed data due to the variance inflation, as in Eq. (9).

Geosci. Model Dev. Discuss., doi:10.5194/gmd-2016-188, 2016
Manuscript under review for journal Geosci. Model Dev.
Published: 31 August 2016

Geoscientific Model Development Discussions

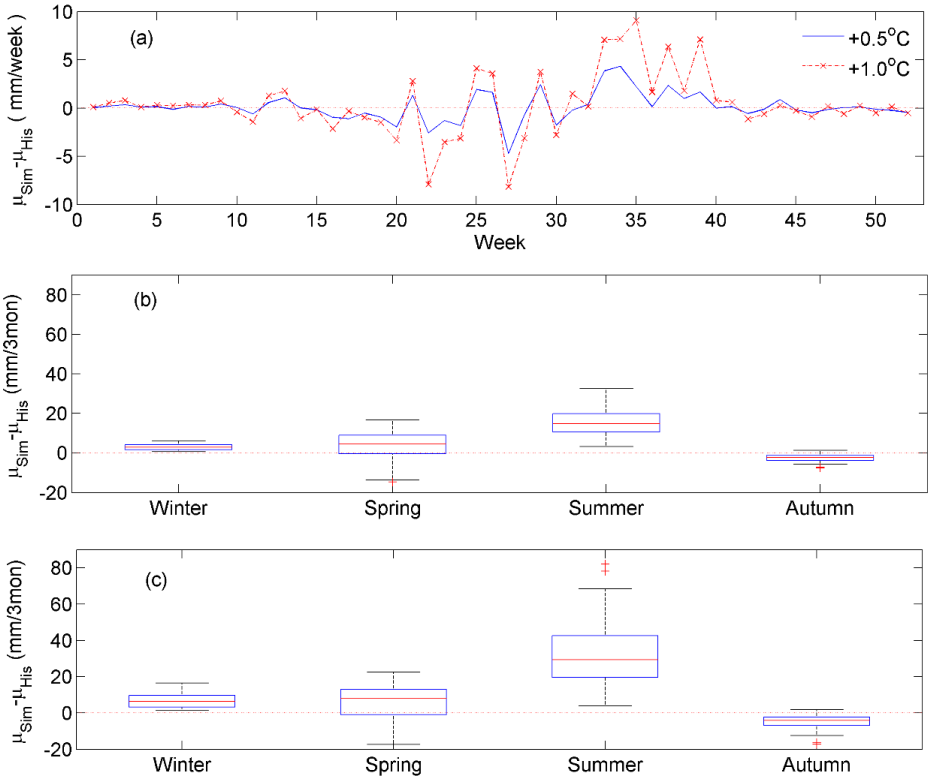

Figure 9. The mean precipitation differences of the observed and simulated data (a) for the weekly precipitation in Buan with a 0.5°C mean temperature increase, (b) for the seasonal precipitation of all 54 stations with a 0.5°C mean temperature increase and (c) for a 1.0°C mean temperature increase. Note that indicates the mean of the simulated precipitation data for weekly (a) or seasonal (b and c).

Geosci. Model Dev. Discuss., doi:10.5194/gmd-2016-188, 2016
Manuscript under review for journal Geosci. Model Dev.
Published: 31 August 2016

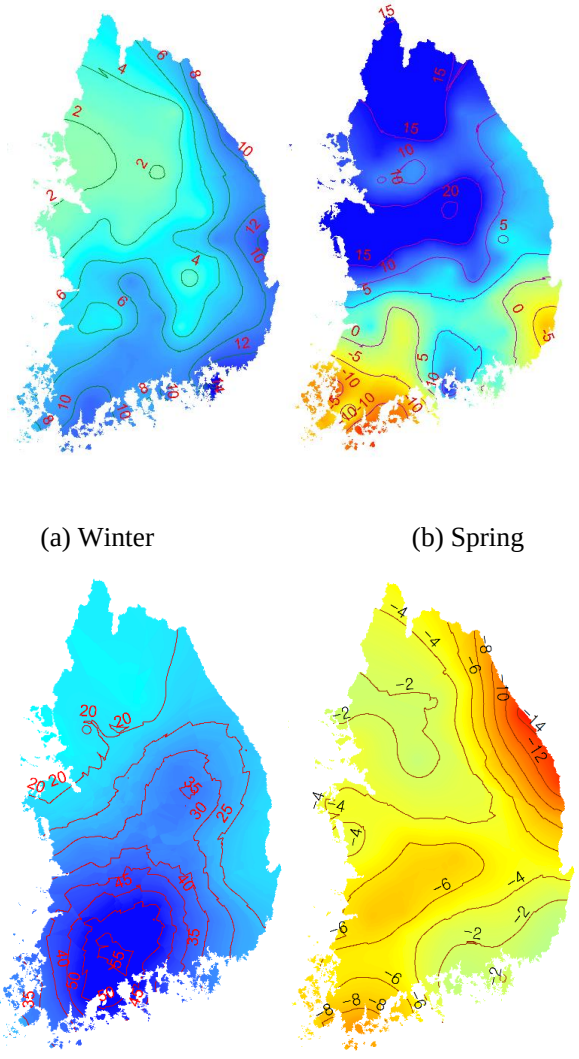

(a) Winter (b) Spring

(c) Summer (d) Autumn

Figure 10. Spatial distributions in South Korea of the mean difference in seasonal precipitation (mm) with a 1.0℃ increase in mean temperature. Note that the scale for the summer distribution is different from the other seasons, the 95% significance intervals are different at each station and the mean values of the significance intervals are ±5.38, ±15.04, ±29.94, and ±4.84 for Winter (December, January, February), Spring (March, April, May), Summer (June, July, August), and Autumn (September, October, November), respectively.

Geosci. Model Dev. Discuss., doi:10.5194/gmd-2016-188, 2016
Manuscript under review for journal Geosci. Model Dev.
Published: 31 August 2016

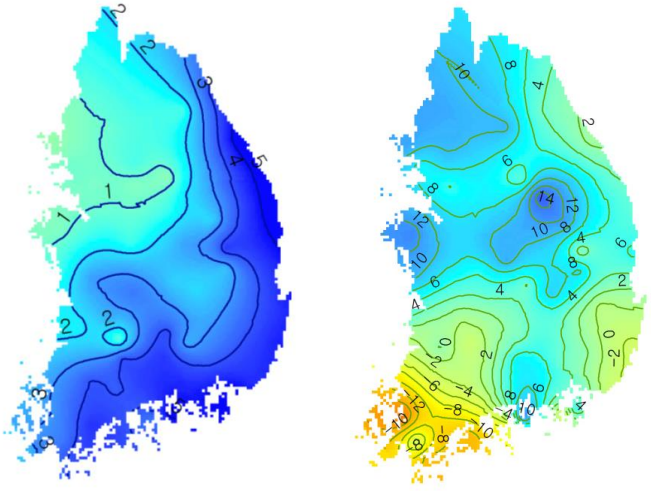

(a)Winter (b)Spring

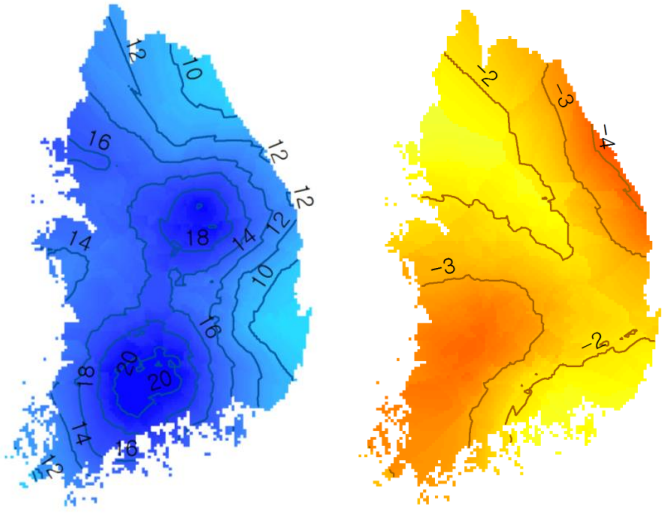

(c)Summer (d)Autumn

Figure 11. Spatial distribution of mean difference of seasonal precipitation (mm) with 0.5ºC increasing mean temperature in South Korea. Note that the scale of summer is different from the other seasons and the 95% significance intervals are different at each station and the mean values of the significance intervals are ±5.38, ±15.04, ±29.94, and ±4.84 for Winter (December, January, February), Spring (March, April, May), Summer (June, July, August), and Autumn (September, October, November) respectively.